March 2018

Measuring Radioactivity in Soil and Dust Samples from Japan

Son Nguyen
Worcester Polytechnic Institute

Steven Joseph Franca
Worcester Polytechnic Institute

Thang Duc Pham
Worcester Polytechnic Institute

Follow this and additional works at: https://digitalcommons.wpi.edu/iqp-all

Measuring Radioactivity in Soil and Dust Samples from Japan

An Interactive Qualifying Project Report

Submitted to the Faculty

of the

Worcester Polytechnic Institute

by

Thang Pham

Steven Franca

Son Nguyen

Abstract

A radioactivity map of Cesium-137, a radioactive material emitted from the Fukushima Dai-ichi Nuclear Power Plant, was created by examining 30 soil and dust samples originating from Japan. A Sodium Iodide (NaI) detector measured gamma rays emitted from the samples. Qualitative evaluation of human exposure to radio-cesium in five sets of locations in Japan shows the radioactivity of tested samples. The Fukushima section of one of the Olympic proposed torch route has a 60 times higher activity of Cesium-137 than the activity of the samples from Tokyo.

Acknowledgement

Executive Summary

Overview

On March 11th, 2011, a magnitude 9.0 earthquake hit the Fukushima Prefecture of Japan (AESJ, 2015, p.19). This resulted in major structural damage to the surrounding area. Following the earthquake, a 13-meter tsunami hit the Fukushima Dai-ichi Nuclear Power Plant and disabled the backup the diesel backup power generator and the cooling water pumps needed to keep the Power Plant running in the event of a disaster. Since power restoration was unsuccessful and there was major structural damage caused to the Units by the tsunami, there were high concentrations of nuclear particles released into the air.

The amount of radioactive materials emitted from the Power Plant raised health and environmental concerns to the people living in the areas around the Fukushima Dai-ichi Nuclear Power Plant. In fact, several studies conducted after the accident determined the activity of radioactive isotopes in the environments. These studies around Fukushima provided excellent understanding of the activity of radioactive isotopes in the environment and the health effects on humans.

With the upcoming XXXII Olympiad in 2020 hosted by Japan, it is necessary to look into the radioactivity of Olympic venues as well as tourist attractions in the host cities. Previous studies pose a major gap because they focused on regions that are closer to the Fukushima Dai-ichi Nuclear Power Plant, where the highest concentration of radioactive fallout is located. On the other hand, the radioactivity in other locations in Japan is relatively less studied. Since thousands of athletes and millions of visitors are travelling to Japan for the Olympics, there has been widespread concern from the international community about radiation exposure. Therefore, it is important to investigate the extent of radioactive fallout from the Fukushima Dai-ichi incident.

Project goals and Objectives

The goals of the project were to measure the radioactivity of Cesium-137 in soil and dust samples from Japan and to generate a map that illustrates the activity of Cesium-137 in five locations in Japan. Understanding the radioactivity in Japan soil would help in giving an estimation of human exposure to radioactivity in the studied areas. The primary objectives of this project were to:

- Perform soil sample preparation for measurement, including categorizing, drying and sub-sampling.
- Measure the activity of Cesium-137 in the samples and analyze the radioactivity at different locations in Japan.
- Generate a map to illustrate the radioactivity level in Japan soil.
- Estimate qualitatively human exposure to radioactivity for people living in the studied areas.

Development of methodology

The employment of various study methods and experiment designs helped complete the objectives. Through literature review and discussion with advisors and lab instructors, we were able to develop main steps and setting for our study.

Primarily, we performed preparation for 87 soil and dust samples collected in Japan and transferred to Worcester Polytechnic Institute (WPI). The samples were classified into five categories based on their original location: Tokyo samples, Azuma Sports Park samples, proposed torch route samples, tourist route samples and non-Olympic samples. All the samples were dried and sub-sampled so that their physical conditions were consistent throughout the testing phase. From the 87 samples that are dried and sub-sampled, we eventually further narrowed to 30 samples for radioactivity measurement.

Previous studies on radioactive nuclides accumulation in soil and dust samples from Japan identified that Cesium-137 had the highest concentration among radionuclides in Japan soil (Saito et al., 2015). Therefore, we set our goal to measure the activity of Cesium-137 in the samples from Japan. A thallium-activated sodium iodine detector, or NaI (TI) detector, measured the concentration of Cesium-137 in the soil samples. The calibrating sources used for Cesium-137 measurement were Cesium-137, Sodium-22 and Manganese-54. The experiment reported the radioactivity of the background and the radioactivity of Cesium-137 in the samples above the background. Measurements were made in triplicate to provide counting variability statistics.

At the beginning of the project, samples were selected randomly for measurement. Our focus then shifted, as we looked deeper into the four main areas that will be important to the XXXII Olympiad in 2020. These Olympic areas included Azuma Sports Park, tourist attractions in Tokyo, a proposed torch route, and official designated tourist routes. Time constraint and large amount of samples, limited testing which resulted in results on only a limited part of each sample set.

After finishing measuring, the radioactivity of the soil and dust samples helped generate a map that shows the activity of Cesium-137 in Japan soil. Since there was a large variation in the measured activity between samples at different locations, we decided to analyze the results based on the samples' original locations.

Our results were cross-referenced with information and results gathered from literature reviews. Understanding the activity of Cesium-137 in Japan soil, we were able to give a qualitative estimation of human exposure.

Results and Analysis

By the end of the project, we were able to measure the activity of Cesium-137 in 30 soil and dust samples. The results showed a great variation in radioactivity between samples from different locations. The activity of Cesium-137 in the 30 samples ranged from 38.6 Bq/kg to 28041.5 Bq/kg with the mean radioactivity of 4903.3 Bq/kg (standard deviation, σ= 6611.0 Bq/kg).

Among the five categories of locations, the Tokyo sample set had the lowest radioactivity mean of 117.6 Bq/kg. The following locations are ordered by increasing mean of radioactivity: Azuma Sports Park samples (2703.9 Bq/kg), main tourist routes samples (3206.0 Bq/kg) and proposed torch route samples (7896.0 Bq/kg). Only one of the non-Olympic samples, which

originates from the Entrance to Fukushima Dai-ichi waste mounds, had a radioactivity of 14119.8 Bq/kg. Due to this outlier, this sample set was omitted from the other sets.

The measured results showed that the Tokyo sample set had the lowest radioactivity level, which was understandable based on its significant distance from the Fukushima Nuclear Power Plant. On the contrary, the proposed torch route samples had the highest mean radioactivity due to their close proximity to the plant. Based on the measurement, we estimated qualitatively that the radiation exposure of people living near the Azuma Sports Park area was 20.7 times higher than that of people living in Tokyo. The main tourist and proposed torch routes had radiation exposure of 24.6 and 60.6 times higher, respectively, than in Tokyo.

The results in this study were in agreement with published results qualitatively. Saito et al. reported a much higher deposition of Cesium-137 in the area to the northeast of the Fukushima Nuclear Power Plant and the further away from the plant, the lower the deposition of Cesium-137 (2015). Accordingly, our results showed that the highest radioactivity level was at the proposed torch route, which is located to the northeast of the plant. The further away from the plant for example, in Tokyo and the Azuma Sports Park, the lower the activity of Cesium-137. However, because of the differences in sampling techniques and reported unit of radioactivity, there could not be an established direct comparison.

Recommendations

Given the aforementioned results, there is significant evidence through our testing, that there are still high amounts of radiation in areas close to the Fukushima Prefecture. Past and current tests found that high amounts of radiation remain at the origin of the disaster. The results showed a significantly higher amount of radioactive materials in the proposed torch route compared to those in Tokyo.

Given the results from testing, we confidently make the following recommendations:
1. Further study on the activity of Cesium-137 on the proposed torch route is necessary to understand how much radioactive materials remain.
2. A more detailed study with more soil and dust samples can give a more accurate map of specific areas of interest.
3. Olympic officials should consider using the results of this project to decide whether the radioactivity level at the proposed torch route and the Olympic venues are within acceptable level.
4. Qualified health professionals should use this data to make connections about short and long-term effects on health.

Authorship

	Primary Author(s)	Primary Editor(s)
Abstract	Steven/Thang	All
Acknowledgement	Steven	All
Executive Summary	All	All
Introduction	Steven/Thang	All
Background		
Fukushima Dai-ichi nuclear disaster	Steven	All
Radiation	Thang	All
Locations of Interest	Son	All
Methodology		
Objective 1: Prepare soil samples for measurement	Thang	All
Objective 2: Measure the radioactivity of Cs-137 in the samples	Thang	All
Objective 3: Generate a map to illustrate the radioactivity level of Japan soil	Thang	All
Findings		
Finding 1	Thang	All
Finding 2	Thang	All
Finding 3	Thang	Thang
Discussions and Recommendations		
Discussion	All	All
Limitations of methodology	Son/Thang	All
Summary	All	All
Recommendation	Steven	All
Appendix	All	All
Other tasks		
Samples preparation	All	
Sample radioactivity measurement	All	
Maps creating	Thang	
Report formatting	Son	

Table of Contents

List of Figures

List of Tables

1. Introduction

On March 11th, 2011, a magnitude 9.0 earthquake hit the Fukushima Prefecture of Japan (AESJ, 2015, p.19). Following the earthquake, a 13-meter tsunami hit the Fukushima Dai-ichi Nuclear Power Plant and disabled the diesel backup power generator and the cooling water pumps needed to keep the Power Plant running in the event of a disaster. Since power restoration was unsuccessful and there was major structural damage caused to the reactor units by the tsunami, there were high concentrations of nuclear particles released into the air.

The amount of radiation emitted from the Power Plant raised health and environmental concerns to the people living in the areas around the Fukushima Dai-ichi Nuclear Power Plant. In fact, several studies conducted after the accident determined the activity of radioactive isotopes in the environments. These studies investigated the transportation of radioactive materials in the atmosphere to the deposition of radioactive nuclides in Japan soil. Morino et al. used a chemical transport model to simulate the transport and deposition of Iodine-131 and Cesium-137, estimating that approximately 13% of Iodine-131 and 22% of Cesium-137 emitted from the Nuclear Power Plant were distributed in Japan soil (2011). Yasunari et al. measured the deposition of Cesium-137 in Japan soil and created a radiocesium deposition map, showing that Cesium-137 was highly deposited in eastern and northeastern of Japan (2011).

More recently, Saito et al. measured the deposition of radioactive nuclides in 10,915 soil samples within 100 km from the Fukushima Dai-ichi Nuclear Power Plant and concluded that the amount of radioactive cesium was much higher than other radioactive nuclides (2015). Kaltofen et al. isolated and analyzed the activity of radiocesium in 180 dust and soil samples from Japan, showing a high mean radioactivity of 25.7 kBq/kg among the sample set (2017). These studies around Fukushima provided excellent understanding of the activity of radioactive isotopes in the environment, which can translate into health effects on humans.

With the upcoming Games of the XXXII Olympiad in 2020 hosted by Japan, it is necessary to look into the radioactivity of Olympic venues as well as tourist attractions in the host cities. Previous studies pose a major gap because they focused on regions that are closer to the Fukushima Dai-ichi Nuclear Power Plant, where the highest concentration of radioactive fallout is located. On the other hand, the deposition in other locations in Japan is relatively less studied. Since thousands of athletes and millions of visitors are travelling to Japan for the Olympics, there has been widespread concern from the international community about radiation exposure. Therefore, it is important to investigate the extent of radioactive fallout from the Fukushima Dai-ichi incident.

In this study, we addressed this concern by measuring the activity of Cesium-137 in 30 soil and dust samples from tourist attractions and Olympic venues in the Fukushima Prefecture and in Tokyo. Some of the noteworthy locations include the Imperial Palace, Azuma Sports Park, as well as various points in the Olympic proposed torch route and tourist route intersecting the Fukushima prefecture.

The goals of this project were to measure and document the radioactivity of soil and dust samples from Japan, generate an activity map of Cesium-137 in Japan soil, and qualitatively estimate human exposure to Cesium-137 among the five locations. A sodium iodide (NaI) detector with ProSpect® software analyzed the data from radioactive measuring of the soil and dust samples. Using Google Maps, a map shows the Cesium-137 activity in the samples.

Cesium-137 was the only radionuclide studied because it has the longest half-life among the emitted radioisotopes from the Fukushima Nuclear Power Plant and is the highest deposited radioisotope (Saito et al., 2015).

The measured radioactivity of soil in Japan from the study can be used as a database for further interpretation in choosing suitable locations for the Olympic.

2. Background

This chapter gives background details around the Fukushima Dai-ichi Nuclear Power Plant disaster, which occurred in 2011. Details give how much emitted radiation occurred in the following months. Other areas of discussion include the basics to radioactive terminology used in the paper, the methods used to test the samples gathered from Japan and previous studies on radiation emitted from the Nuclear Power Plant. Finally, information about the samples' location of origin discuss the importance of those areas.

2.1 Fukushima Dai-ichi Nuclear Disaster

Fukushima City is located in the Fukushima Prefecture, which has an area of 5,320 mi; Japan's third largest out of 43 total prefectures. It is located on the South Eastern part of the country and is perfect for shipping routes especially in the coastal region of Hokkaido and Tohoku. Currently there is around 1.9 million people living in the entire Fukushima area. (Future From Fukushima, 2018) The weather makes this region comfortable to live in and is not susceptible to many natural disasters; only small, undisruptive earthquakes are common to the country of Japan. Around the city of Fukushima, mountainous areas and many national parks attract many tourists to this vibrant area (Jnto Japan: The Official Guide).

Since this prefecture expands to the coastline, the Fukushima Dai-ichi Nuclear Power Plant commissioned in 1971, thrived off being close the water and located far from any major cities. The power plant, comprised of six reactors, generating around 4.7 million kW, which is a significant portion of the total energy generated in the country (INES, 2015, p.7). The oldest unit, Unit 1 and the oldest, Unit 6 have varying differences mainly including function. For example, Unit 6 has more efficient jet pumps to allow for better water circulation that in Units 4 and 5.

At 14:46 JTC on Friday March 11th 2011, a magnitude 9 earthquake originating near the towns of Naraha and Tomioka, triggered a chain of events that would ultimately result in a level 7 nuclear event (INES, 2015, p.19). The earthquake itself only prompted the automatic shutdown of the fission reactions at the active reactors. This is the fourth largest earthquake recorded in world history.

In 1990, the International Atomic Energy Agency (IAEA) introduced the International Nuclear and Radiological Event Scale (INES), which gives a scale on how much response and protocol is associated to a particular nuclear event. This scale range from zero to seven. A zero on the scale simply refers to a lack of breach of safety. A one on the scale refers to an anomaly, which corresponds to a leak of nuclear particles contained only in a small area, which does not cause much harm (INES, 2017). In the case of Chernobyl and the Fukushima Dai-ichi disaster, they were both rated a seven, which is the highest value on the scale and considered a major threat to safety for workers and people around the area. To give a scale about the different levels, they increase logarithmically which means that every level increase represents a ten times greater severity level (INES, 2017).

First, the earthquake damaged external power supplies, which automatically caused the nuclear reactors to shut down their power. When the power cut, emergency diesel generators activated which restored power to all of the Units except for Unit 4, which was under inspection at the time of the earthquake (INES, 2015, p.19). Not a lot of physical damage to the reactors as reported by officials inspecting the damage.

Around an hour after the earthquake, a tsunami caused by the earthquake hit the coast of Japan. TEPCO reported that the height of the tsunami was around 13 meters (AESJ, 2015, p.20). Warnings issued in the area alerted citizens to prepare for incoming water. As the seawater entered the land, the Fukushima Dai-ichi Nuclear Power Plant Units flooded. In turn, the power cut and could not be restored. Emergency plans included rerouting power and generation power for the plants off site but the water damage was critical enough to render those plans useless. In addition, debris from affected structures hindered any help. This massive tsunami ranked as fourth largest in recorded history. Over the span of 3 days from March 12th to March 15th, the cores in Unit 1, 2 and 3 melted and released radioactive particles in the environment (AESJ, 2015, p.222). These radioactive particles not only spread all over Japan, but also spread to adjacent countries as well as in the ocean. Unit 2 caused the most damage because damage to the structure itself allowed the escape of particles into the atmosphere (AESJ, 2015, p.31).

2.1.1 Radiation Testing Results

Air tests revealed that the areas around Fukushima, around 24 km from ground zero, experienced a spike in μSv/h. The highest reported reading was around 24 μSv/h (AESJ, 2015, p.75). To give perspective, 100 μSv/h will give heightened sickness risk and 20 μSv/h will give sickness risk (Shoebridge, 2012). Both of these, considered high danger. To be considered safe, the reading had to be around 1 μSv/h. At around 5 μSv/h, there is an elevated risk and relocations are suggested (Shoebridge, 2012). 10 days after the earthquake, the levels ranged from around 3 μSv/h to 7 μSv/h (AESJ, 2015, p.75).

2.1.2 Radiation Standards for Consumption

In Japan, there are standards for the concentration of radiation in food allowed in the country. In 2012, these standard values were reduced and the current value is 100 Bq/kg (Stefan Merz, Katsumi Shozugawa, and Georg Steinhauser; Analysis of Japanese Radionuclide Monitoring Data of Food Before and After the Fukushima Nuclear Accident; Environ. Sci. Technol. 49, 5, 2875-2885).

During any major disaster, the government has a responsibility to keep its citizens safe by taking the right precautions and following procedures. The main responsibilities include effectively moving resources to help with relief and conducting the proper research, which will in turn cause less harm to workers and reduce damage in general. The licensee operating any nuclear power plant can sufficiently fulfill the government's rules and regulations, but it does not mean that those rules are sufficient for the safety of the power plant. These regulations are not always the most current and with ever changing technology, we get a barebones outline of how a licensee can ignore many risk factors that the government's rules do not cover. It is easy for them to not take further action to improve upon safety.

2.1.3 Aftermath

During the disaster, as expected, the government issued warnings of a possible tsunami in the area, which just experienced the earthquake. Response teams executed the procedures in the event of a nuclear meltdown from the Fukushima Dai-ichi Power Plant. Around six hours after the earthquake hit, the Governor of Fukushima ordered an evacuation of the residents living in the towns where the earthquake's origin was. At the start of the evacuations, a 3 km radius was

designated. By the next day, the evacuation radius grew to 20 km because of the severity of the events. At the peak of the incident, the radius grew to 30 km around the Fukushima Dai-ichi plant because wind and air carried particles to the surrounding area (AESJ, 2015, p.323).

Fortunately, for the citizens in the Fukushima Prefecture, there were no casualties resulting from the Fukushima Dai-ichi nuclear meltdown. However, long-term effects from radiation exposure are possible. Thyroid cancer in children is a concern. With the 2020 Summer Olympics set in Tokyo, Japan, a major focus is to examine if the areas designated for the games is safe for the athletes, staff, and all in attendance. Furthermore, with a proposed torch route and some of the events set to be held in parts of the Fukushima Prefecture it is our group's primary concern to look into the samples of origination from the aforementioned locations first.

2.2 Radiation

2.2.1 Overview

Radiation is the emission or transmission of energy in the forms of waves or particles through space. There are four types of radiation: Charged particulate radiation (including Fast electrons and Heavy charged particles) and uncharged radiation (including Electromagnetic radiation and Neutrons). A more detailed description for each category of radiation can be found in "Radiation Detection and Measurement" (Knoll, 2010).

Our project studied gamma radiation, a source of Electromagnetic radiation.

2.2.2 Radioactivity Measurement

Radioactivity, or the activity of a radionuclide, is the rate of decay. A radionuclide (radioisotope) is an atom that possesses excess nuclear energy and thus is unstable. The International System of Units (SI) unit for radioactivity measurement is Becquerel (Bq), defined as one disintegration per second.

Different radiations have different energy levels. The traditional unit for radiation energy measurement is electron volt (eV).

2.2.3 Gamma Radiation

Gamma radiation, or gamma ray, is a penetrating electromagnetic radiation. Gamma radiation is often emitted during radioactive decay when a parent radionuclide decays to a daughter nucleus that initially exists in an excited state. This decay released gamma ray photon with an energy equal to the difference between the two energy states. Because different radioisotopes release gamma rays at different energy levels, identification of the radioisotope uses the comparison of its gamma radiation energy to literature values. For example, ^{137}Cs, the radionuclide of interest in this project, emits gamma photons of 662 keV. For other radioisotopes, the typical energy for gamma ray radiation is above 100 keV.

Four common widely used calibration sources are $^{22}_{11}Na$, $^{57}_{27}Co$, $^{60}_{27}Co$ and $^{137}_{55}Cs$ (Knoll, 2010). Their absolute gamma emission rates are depicted in the decay diagrams below.
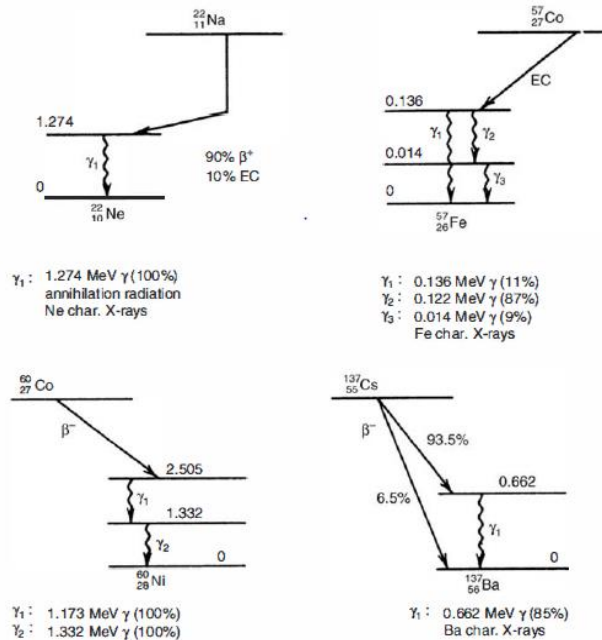
Figure 1: Gamma radiation emission rate for four common calibration sources. (Knoll, 2010)

To illustrate, in Fig. 1, the 0.662 MeV gamma photon is only observed during 85% (not 100%) of Cesium-137 decay because of a competing de-excitation mode for the excited Barium-137 nucleus.

The four main radionuclides emitted from Japan include [137]Cs (half-life 30.17 years), [134]Cs (half-life 2.06 years), [131]I (half-life 8.02 days), [129m]Te (33.6 days) and [110m]Ag (249.79 days). Because this project was conducted more than 6 years after the Fukushima disaster, our study aimed to measure the radioactivity of only ^{137}Cs in soil samples because its half-life is the highest and it was reported to be the most abundant radionuclide emitted from the Fukushima Nuclear Power Plant.

2.2.4 Previous Studies

Several studies indicate the distribution and deposition of gamma ray emitting radionuclides from the Fukushima Dai-ichi Nuclear Power Plant. The topics of these studies range from the radionuclide transport in the air to the deposition in water and soil. Morino et al. (2011) used the chemical transport model to study the deposition of radioactive materials in the air after the Fukushima disaster. Nagao et al. studied the export of [134]Cs and ^{137}Cs in the Fukushima river systems, showing that rain events are one factor contributing to the transport of radiocesium in the river (2012). Saito et al, analyzed 10,915 soil samples to study the deposition of gamma-ray emitting radioactive nuclides in the soils within 100 km from the Fukushima Nuclear Power Plant (2015). The large of number of studies on radionuclides from the disaster have shown the public's concern on human health and environment. Among the articles studying on deposition of radionuclides in the soil, there were two main approaches: one concentrating on the depth distribution of deposited radionuclides in the soil, the other focusing on the deposition of radionuclides on the surface of the soil. These studies around Fukushima provided excellent

understanding of the activity of radioactive isotopes in the environment, which can translate into health effects on humans.

In the former category, Tanaka et al. studied the vertical profile of ^{131}I and ^{137}Cs in soil in Fukushima prefecture (2011). Their results showed that highest distribution of the Iodine and Cesium radionuclides occur close to the surface at depths of 0 to 5 cm, suggesting that studying the deposition of ^{137}Cs on the surface soil could be more important than the depth distribution.

In the latter category, Yasunari et al (2011) estimated the distribution of ^{137}Cs in Japan soils due to the Fukushima nuclear accident using Lagrangian particle dispersion model. Kinoshita et al. (2011) measured the concentration of five radioisotopes (^{137}Cs, ^{136}Cs, ^{134}Cs, ^{131}I, ^{129m}Te and ^{110m}Ag) in the soil using a high pure germanium detector. Saito et al. (2015) showed that the four main radionuclides emitted from the Nuclear Power Plant are ^{137}Cs, ^{131}I, ^{129m}Te and ^{110m}Ag. The study concluded that the radiation doses from radioactive Cesium were found to be much higher than those from other radioisotopes. Kaltofen et al. isolated and analyzed the activity of radiocesium in 180 dust and soil samples from Japan, showing a high mean radioactivity of 25.7 kBq/kg among the sample set (2017).

2.3 Locations of Interest

2.3.1 Overview

To examine the effect of nuclear fallout from the Fukushima accident, our research looked into dust and soil samples collected from the Fukushima prefecture as well as regions that are relatively far away from the Fukushima Dai-ichi site. Specifically, our team chose to focus on samples collected from the Fukushima prefecture as well as the Tokyo prefecture. Among our locations of interest were the Azuma National Sports Park which is the Olympic baseball stadium, the Imperial Palace of Tokyo, the Meiji Shrine, and several sites in the Fukushima prefecture that are going to be parts of a possible Olympic proposed torch route. Regarding our choice of sample, the Fukushima prefecture was an obvious choice due to its vicinity to the original site of the meltdown, the Fukushima Dai-ichi Nuclear Power Plant. On the other hand, we chose to investigate samples in the Tokyo prefecture and specifically, Tokyo city, because we wanted to examine whether regions that are relatively far away from Fukushima are in the range of the nuclear fallout from the Fukushima-Fukushima Dai-ichi accident. Furthermore, Tokyo city was an important choice due to its importance as the capital of Japan and one of the world's busiest and most populous city. Another thing that we were primarily mindful of was that Tokyo is also one of Japan's prime tourist destination as the city welcomed nearly 12 million visitors in just 2015 alone.

More importantly, it is worth noting that the 2020 Summer Olympic will be primarily held in Tokyo with some minor softball and baseball preliminary games held in Fukushima. Thus, an already impressive number of tourists visiting Tokyo is only going to increase and Fukushima city will also see an uptick in the number of tourists visiting as well come to the Olympics games in 2020. This uptick influenced our decision to look into samples from Tokyo and Fukushima. To be more specific, the Azuma National Sports Park, located in the Fukushima Prefecture, is going to be the venue for baseball and softball games. Meanwhile, the Imperial Palace in Tokyo and the Meiji Shrine, aside from being a top-rated tourist attraction, are

also included in the "heritage zone" that will be used as part of the cycling route for the Olympics.

2.3.2 Imperial Palace of Tokyo

Our first location of interest was the Imperial Palace of Tokyo or 皇居 in Japanese, a location of great importance and prestige in Japan as well as one of Tokyo's most popular tourist attraction. The Imperial Palace of Tokyo, also known as the Imperial Residence, as its name suggested is comparable to Japan as the Buckingham Palace is to Britain. Not only is the Imperial Palace of Tokyo of great historical significance it is the residence of the Emperor of Japan, his consort, the Empress and their extended family, and all 19 members of the Imperial Family. Built on the site of the old Edo Castle, which traced its origin way back to the Tokugawa Shogunate, the Imperial Palace bore witness to Japan's decline during the Second World War as well as the country's resurgence during the modern era (JNTO, 2014). Moreover, the Imperial Palace of Tokyo is an extremely foot trafficked landmark that attracts hundreds of thousands of tourists every year as well (Kyodo, 2015). With most of the Olympic Games held in Tokyo, the number of tourists that are going to visit the Imperial Palace of Tokyo will increase substantially come the Olympics. Most importantly, as part of the 2020 Olympics, the Imperial Palace is also going to host Olympic venues for the cycling competitions.

2.3.3 Azuma National Sports Park

Another location of interest was the Azuma National Sports Park. The National Sports Park is in Fukushima city. The Stadium itself can contain about 6000 spectators, and the organizer expects that most of these seats to be filled by the time the Olympic torch is lit in Tokyo. Since some of the preliminary baseball and softball games held at the Azuma National Sports Park in the Fukushima Prefecture, the Japanese government wished to show the world that this region as a whole has entirely recovered from the Fukushima Dai-ichi incident and now safe to inhabit. Although the Azuma National Sports Park is located within the Fukushima prefecture, it is located 90 km northwest of the Fukushima Dai-ichi nuclear power plant.

2.3.4 Olympic Proposed Torch Route Passing Through the Fukushima Prefecture

Our last location of interest was the area in the Fukushima prefecture that is going to be part of the Olympic proposed torch route. Compared to other two sites, these areas are neither tourist attractions nor places of great importance and historical significance. These locations remain of great interest because some points are relatively close to the Fukushima Dai-ichi plant. Furthermore, this area is also close to the mountain range in the Fukushima prefecture where most of the prefecture's natural water resources are located. More importantly, this area is also close to farmland that produces vegetables and plants for local and exported use. This is a good reason to look into the samples collected here to see whether the agriculture areas in the Fukushima prefecture has nuclear fallout and radioactive material.

3. Methodology

The goals of the project were to measure the radioactivity of Japan soil, to document the results and to generate a map that illustrates the soil radioactivity level at different locations in Japan. To accomplish these goals, a list of objectives was set to follow:

1. Prepare soil samples for measurement.
2. Measure the radioactivity of ^{137}Cs in the samples and analyze the results.
3. Generate a map to illustrate the radioactivity level.

3.1 Prepare Soil Samples for Measurement.

3.1.1 Overview

Eighty-seven samples originate from Japan in 2017, which is 6 years after the Fukushima Dai-ichi nuclear disaster. Of the 87 samples, 35 were street dirt and dust, and 52 were surface soils and sediments. Due to the variety of locations and weather conditions, the samples arrived at different physical conditions (wet, dry, weight, etc.). Therefore, samples were prepared to have similar physical conditions, which would ensure consistent radioactivity measurement.

3.1.2 Sample Classification

The samples were first classified into five categories based on their original locations and Olympic purposes.

- Tokyo sample: Samples collected from Tokyo, including samples from the Imperial Palace and Meiji Shrine.
- Azuma Sports Park sample: Samples collected from a baseball court in the Azuma National Sports Park in Fukushima city.
- Olympic proposed torch route sample: Samples collected on routes for an Olympic proposed torch route.
- Tourist route sample: Samples collected from main routes taken by tourists to different Olympic locations.
- Non-Olympic sample: Samples collected on road or sites unrelated to the Olympic events.

3.1.3 Sample Drying

More than 60 percent of the samples arrived in wet condition. The wet samples were open to the ambient air (62.2 °F, 22% humidity and 1 atm) in one week to ensure dehydration. Once these samples were dried, their dry net weights were measured using the following formula:

$$m_{dry,\ net} = m_{dry,\ total} - m_{bag}$$

Where: $m_{dry,\ net}$ is the dry net weight of the soils, $m_{dry,\ total}$ is the dry weight of the sample (including the bag) and m_{bag} is the average mass of the bag.

3.1.4 Sub-sample Creation

The 87 samples arrived at different weight, and the difference in weight could generate variance in the radioactivity measurement. Therefore, to eliminate the possible variance arising from the sample size, we created sub-samples from the original samples. After the wet samples was dried, sub-samples were created. The ideal weight of the sub-samples were 8 ± 0.6 grams. The value of 8 grams was determined to be suitable for the measurement because of two reasons: 1. Approximately 25 percent of the samples were at this size so the effort to make sub-sample was reduced and 2. At 8 grams, the sample spread evenly on the detector surface, giving higher geometric efficiency and thus better measurement.

Samples that were smaller in size (dry net weight less than 8 grams) measured directly without being sub-sampled.

By creating sub-samples, we ensured that the collected radioactivity was consistent in all measurement. A drawback is the chance of the removal of radioactive particles from the original samples, thereby lowering the true radioactivity.

3.2 Measure the Radioactivity of Cs-137 In the Samples

Numerous studies have shown that the emitted radionuclides after the Fukushima disaster included ^{137}Cs (half-life 30.17 years), ^{134}Cs (half-life 2.06 years), ^{131}I (half-life 8.02 days) and ^{129m}Te (half-life 33.6 days). Of these radionuclides, Saito et al. reported that ^{137}Cs had the highest concentration in soils (2015). Moreover, because this study was conducted 6 years after the Fukushima nuclear disaster, and only ^{137}Cs has a half-life higher than that, measuring the activity of ^{137}Cs in the soil was expected to yield detectable activity.

This section described the lab set up, the measurement procedure, and data analysis.

3.2.1 Lab Setup

a. Equipment

The information for the equipment was described in the Nuclear Lab Manual (DelSignore, 2017). Here is the summary of the main details for the equipment in the manual. The thallium-activated sodium iodide detector, or NaI (TI) detector was used for the measurement. Photos of the detector are shown in Appendix B.

The detector has sodium iodide (NaI) as the scintillating crystal, which emits visible or ultraviolet (UV) light after absorbing ionizing radiation. The detector used in this study contains a 3-inch diameter by 3-inch tall cylindrical NaI crystals. The light photon hits the photocathode, which is made of a material that emits electrons when struck by visible light photons. The electrons ejected from the photocathode are then multiplied in the photomultiplying tube (PMT), which generates a signal multiplication for an electron leaving the photocathode. The pre-amplifier, which is in close proximity to the signal output of the PMT, captures the current-signal and converts it into a voltage pulse. An amplifier for further amplification and pulse shaping then collects the voltage pulse. The amplifier's job is to produce an output voltage pulse proportional to the charge deposited in the PMT. The output is recorded and analyzed by the multi-channel analyzer (MCA) and Pulse Height Analysis (PHA). The MCA channel contains an analog-to-digital converted, a memory with storage location, control circuity and a timer. The MCA

channel number was 2048. As pulses are collected, PHA, which is a histogram of recorded spectrum, can be created and shown in the ProSpect® software.

b. Detector Efficiency

Since the scintillator surface does not have a uniform efficiency distribution, the measurement for each sample will vary if the sample is put at different parts on the surface of the NaI detector. Therefore, an efficiency profile of the NaI detector surface was analyzed.
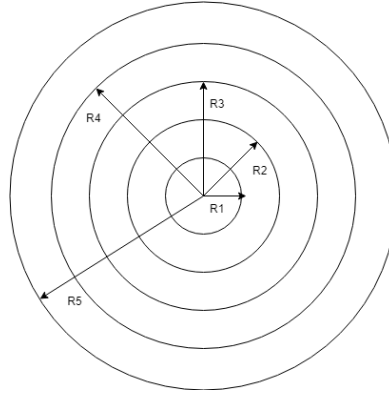

Figure 2: Sodium iodide (NaI) detector surface containing five concentric zones

To develop the efficiency profile, the ^{137}Cs point source was put into a Whirlpak® bag, and the whole container was placed on the detector surface and measured the activity. This setup (with the Whirlpak® bag) was similar to the measurement of an actual sample and made the efficiency profile more realistic. The surface of the NaI detector was divided into five concentric zones (Figure 2), which the radii from the innermost circle to the outermost circle be r, 2r, 3r, 4r and 5r respectively, where r is equal to 0.318 cm. The ^{137}Cs source (in the Whirlpak® bag) was then put at different zones and number of counts at that zone was recorded. The detailed setup for the efficiency measurement is shown in Appendix C.

$$\epsilon_{detector} = \frac{N_c}{\epsilon_{geometry} \times N_p}$$

Where: N_C: Number of counts per second recorded by the detector

N_p: Number of photons incident on detector face

$\epsilon_{detector}$: The detector efficiency for distributed sample on detector surface

$\epsilon_{geometry}$: The geometric efficiency, which depends on the geometry used to measure a sample. Here the assumed $\epsilon_{geometry}$ is 0.5, which the geometric efficiency of a point source lying flat on the detector surface.

Since the container size of the soil sample could vary, developing an efficiency profile for the NaI detector would help determine the detector efficiency for each sample.

c. Experiment setup

The folded size of the measured sub-samples are 3.5 ± 0.4 cm × 3.5± 0.4 cm. The reason for this step was to ensure that the correctly recorded measurement at the high efficiency region. The sub-samples were placed directly on top the surface of the NaI detector.

According to the Nuclear Lab Manual (DelSignore, 2017), each sample's photopeaks must contain at least 10,000 counts for good statistics. Therefore, we ran the radioactivity measurement for the least radioactive sample (based on preliminary results from the sample gatherers) and estimated that three hours would be sufficient to have 10,000 counts for all the samples.

Each sub-sample was measured three times and the number counts (N_c) for each sub-sample was averaged. This step was to ensure good statistics for the results.

In our measurements, the detector remained unshielded. This step measured the radioactivity of the background and considered those in our final calculations. The setup for our measurement is shown in Appendix D.

Table 2 below summarized the details of our measurement.

Measurement criteria	Details for each sample
Sub-sample mass	8 ± 0.6 grams (Samples below 7.4 grams was measured directly)
Sub-sample size	3.5 ± 0.4 cm * 3.5 ± 0.4 cm
Detector efficiency	Based on the detector efficiency profile and sub-sample size
Geometric efficiency	0.5
Number of measurements	Each sample 3 times
Detector shielding	Not shielded

Table 1: Measurement details for each sample

d. Background measurement

Other objects in the lab could generate background noise in the measurements. Therefore, we measured the radioactivity of the background running the measurement with a clean Whirlpak® bag, which was the sample container, on top of the detector surface. The radioactivity of the background was subtracted from the sub-sample measurements to have the corrected radioactivity. The setup for the background measurement is shown in Appendix C, Figure 22.

e. Calibration source

The detector detected the energy level of the soil samples by correctly calibrating the software. Since we aimed to identify the activity of [137]Cs (photopeak: 662 keV) in our samples, three calibrating sources with photopeaks close to that of ^{137}Cs were chosen: [137]Cs, [22]Na (511 keV) and [54]Mn (834.8 keV).

3.2.2 Measurement Procedure

Once the experiment was set up, the ProSpect® software measured the number of counts that the sample generated on the NaI detector surface.

To set up the ProSpect® program, first, in the High Voltage Power Supply window, the reading was turned on and set to be 900 V (Fig. 3).
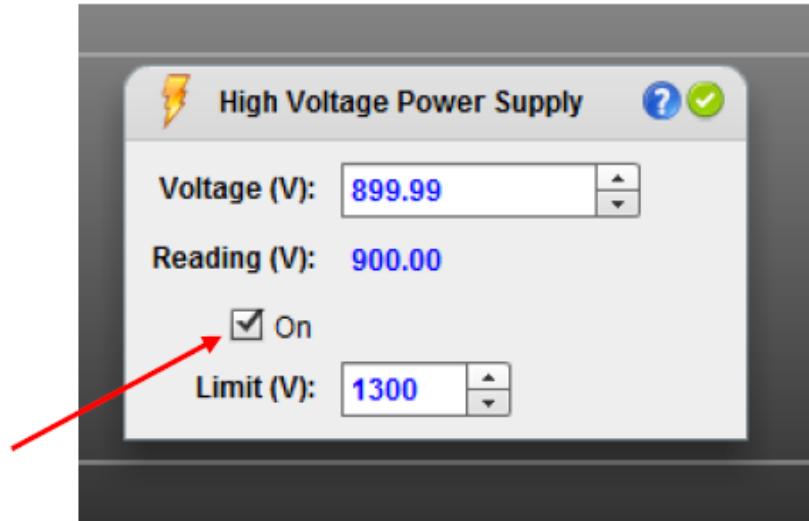

Figure 3: High Voltage Power Supply setting

Next, in the MCA Settings tab, the Coarse and Fine Gain settings were adjusted to optimize the usage of the MCA channels. The setting parameters were shown in figure 4 below.
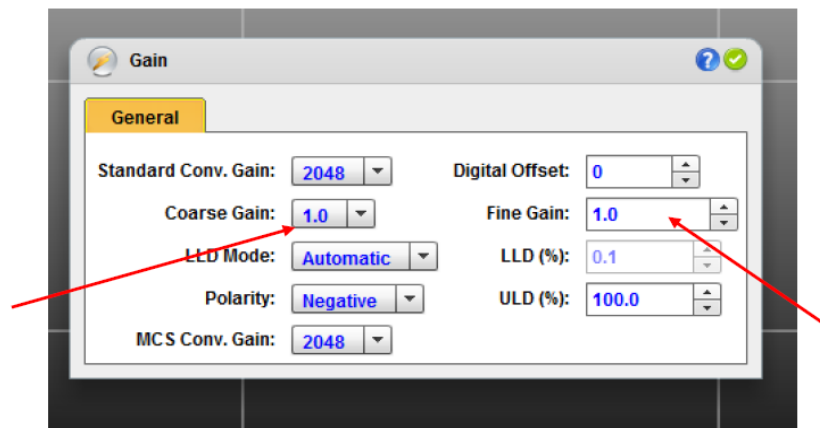

Figure 4: Multi-channel analyzer (MCA) setting

Finally, the detector was set to be pulse height analysis (PHA) mode in the Acquisition tab. The preset counting time was set at three hours as shown in Figure 5.
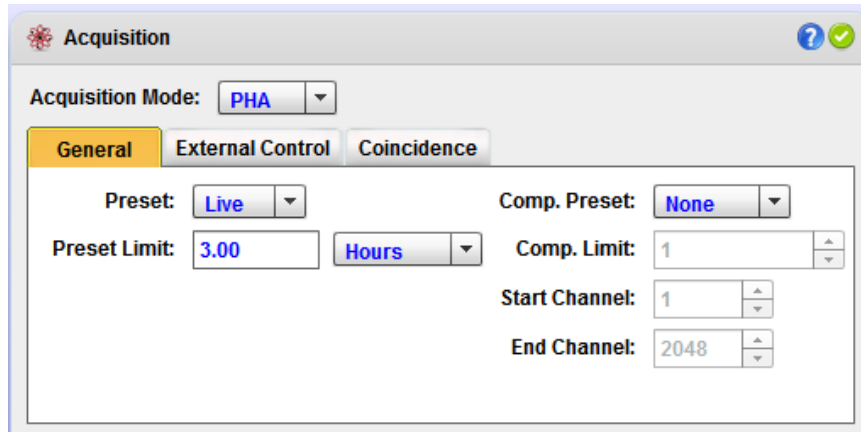
Figure 5: Acquisition setting

Once the measurement finished, the data saved as both .cvs and .ava file. While the .ava file recorded the measurement done by, the .cvs file (Figure 6) was used to calculate the total number of counts in a fixed range of energy, which was used later in our calculation.

Figure 6: Sample of a .cvs file generated by ProSpect®. Data from sample 024S.

The .cvs file showed the details of the measurement, including starting time, measuring time, different energy level and the number of counts detected at that level.

3.2.3 Data Analysis

The actual net count for each sample (C_{net}) used in the equation above was calculated from:

$$C_{net} = C_{gross} - C_{background}$$

Where: C_{gross}: Number of counts for each sub-sample

$C_{background}$: Number of counts for the background

Since the radioactive isotope we aimed to identify is ^{137}Cs, the set chosen energy range lies between 550.03 keV and 700.82 keV , which calculate to number of counts for each sub-sample

and for the background. In other words, C_{gross} and $C_{background}$ was the number of counts between 550.03 keV and 700.82 keV energy range.

The net count per second (CPS_{net}) was calculated from the net count (C_{net}) using the following equation:

$$CPS_{net} = \frac{C_{net}}{T}$$

Where T is the measured time for each subsample in seconds, and T = 10800 seconds in this study.

The disintegration per second (DPS) was calculated using the following equation:

$$DPS = \frac{CPS_{net}}{\epsilon_{detector} \times \epsilon_{geometry}}$$

The activity of each sample was then calculated using the formula:

$$Activity = \frac{DPS}{m_{net}}$$

Where: m$_{net}$: dry net weight for each sample (kg)

3.3 Generating A Map to Illustrate the Radioactivity Level of Japan soil

After accomplishing objective 2, the radioactivity of the samples was plotted on the Japanese map based on their original locations. We chose Google Map because of its convenience in mapping and its nice outlook.

A .cvs file was generated with 7 columns were generated (Figure 7). The named columns include Latitude, Longitude, Name, Description, Icon, AppendataColumnsToDescription, and Activity detected (Bq/kg) respectively.

Figure 7: A sample of the .cvs file used in Google Map.

The first two columns (Latitude and Longitude) contained the location of the sample. The Name, Description and Icon showed the details of the samples. The icon column, left blank,

showed the icon for each sample on Google map. The AppendataColumnsToDescription showed the column that Google map used to create the color-coded radioactivity. The last column, Activity detected (Bq/kg), contained our measured radioactivity.

4. Findings

In this chapter, we described the results for each objective set in the Methodology chapter. The section began with the results of experiment preparation, including our sample preparation and efficiency measurement, then results of the radioactivity measurement and finally the results of our mapping process. We were able to achieve the ultimate goal for this study, which was to generate maps that illustrate the soil radioactivity level at different locations in Japan.

4.1 Sample Preparation and Parameters Measurement

4.1.1 Sample Preparation

a. Sample Drying

Forty-three samples were completely dried in ambient air in the Nuclear Lab (Olin Hall, room 014). Appendix A shows our setup for the drying process

b. Sub-sample Creation

Of the 30 samples that we measured (30 out of 87 samples), the mean net weight of the sub-samples was 6.9 g with a standard deviation (σ) of 2.5 g. The mean net weight was below the ideal weight that we wanted (8 g) because 7 samples were undersized. If the 7 undersize samples were disregarded, the mean net weight for the 23 sub-samples were 8.1 g ($\sigma = 0.36$ g).

4.1.2 Detector Efficiency
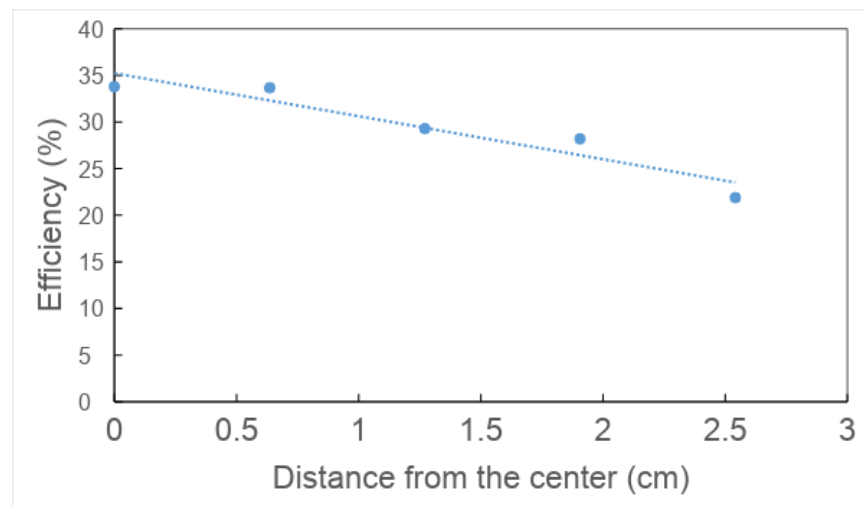
Figure 8: Efficiency profile as a function of distance from the center

The efficiency profile was developed for the surface of the NaI detector. Figure 8 shows a plot of the detector efficiency versus the distance from the center of the detector. The efficiency of the detector was expressed as a quadratic function of the distance from the center of the detector with a high R-squared value of 0.96. The strong dependence of the surface efficiency on

the distance from the center of the detector required our group to calculate the detector efficiency for each sample based on its size.

4.2 Radioactivity Measurement

4.2.1 Background Measurement

The background radioactivity was measured three times and the number of counts within the interested energy range (550.03 keV and 700.82 keV) was averaged. Table 3 showed the total number of counts for the three background measurements in 3 hours.

	Run 1	Run 2	Run 3
$C_{background}$ (counts)	22097	21955	22041

Table 2: Number counts for the three background measurements.

The average number of counts for the background measurements is 22031 counts (σ = 71.5 counts). The differences between each measurement arose because of the radioactive samples within the lab and other groups conducting their measurements nearby. A sample of background measurement is shown is Appendix B.

4.2.2 Control Samples

One soil sample from Worcester Polytechnic Institute (100 Institute Road, Worcester, MA) was measured to example the activity of radiocesium in the soil. The result showed that activity of ^{137}Cs in the sample was 0.0 Bq/kg, confirming that there is no radiocesium in the soil sample at WPI.

4.2.3 Japan soil and Dust Samples Measurement

The radioactivity of the dust and soil samples ranged from 38.6 Bq/kg to 28041.5 Bq/kg. Figure 9 shows the radioactivity of ^{137}Cs in 30 samples (30 of 87 samples) measured in our study. The mean radioactivity of the 30 Japan soil and dust samples was 4903.3 Bq/kg (σ = 6611.0 Bq/kg). The radioactivity data in the study was assumed to be ^{137}Cs and not corrected for ^{134}Cs. Thirty percent of the samples (9 of 30 samples) exceeded the overall mean radioactivity. Of these samples, four (4 of 9) exceeded 11514.3 Bq/kg (mean + 1σ) and one (1 of 9) exceeded 18125.3 Bq/kg (mean + 2σ).

The large standard deviation showed that the radioactivity varied greatly between samples from different locations. Therefore, a detailed analysis of the radioactivity at each location would be discussed in the sequential sections to fully understand the activity of ^{137}Cs in Japan soil.
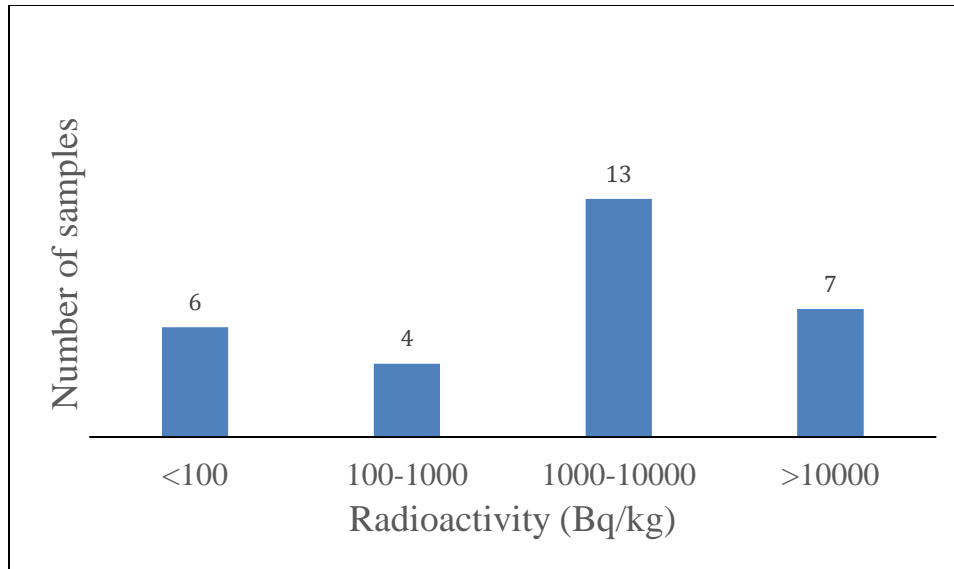
Figure 9: Histogram showing the number of soil samples from Japan by order of magnitude of radioactivity of ^{137}Cs in Bq/kg.

4.3 Japan Soil Radioactivity Maps

Once we calculated the radioactivity of the samples, we created maps that shows the radioactivity level of soil in Japan. This section explored the overall radioactivity level of Japan soil and went into details for each sample categories.

4.3.1 Overall Heat Map

Figure 10 showed the radioactivity of ^{137}Cs in Japan soil. Every soil samples were measured three times and the average radioactivity was reported and mapped. The general trend was that the further away from Fukushima Nuclear Power Plant, the lower the radioactivity of ^{137}Cs in the samples.

While the samples from Tokyo set showed the least activity of ^{137}Cs, samples from the proposed torch route set showed much higher activity.
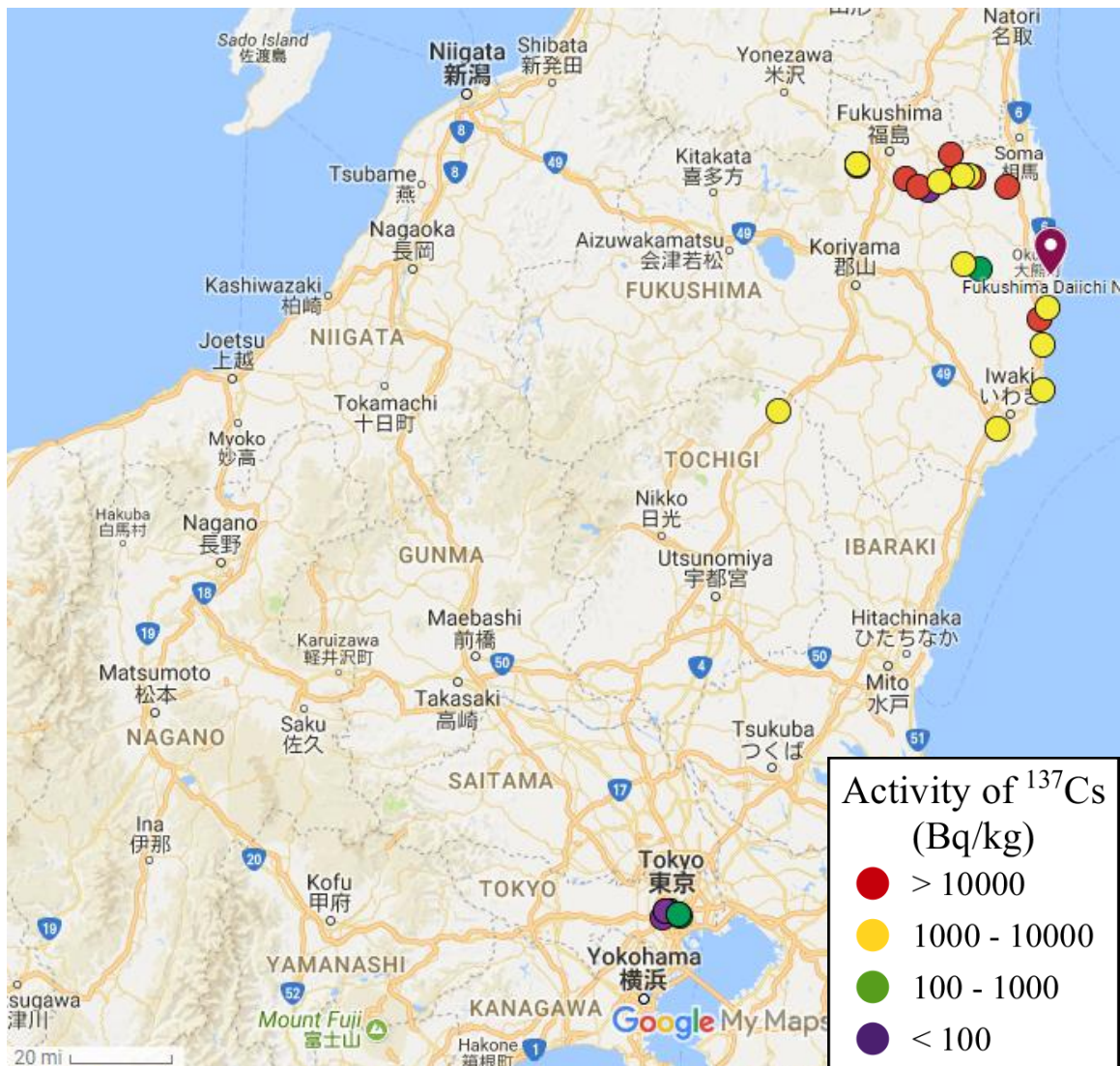
Figure 10: Overall activity of ^{137}Cs in Japan soil and dust samples.

4.3.2 Tokyo Sample

Figure 11 showed the overall activity of ^{137}Cs in Tokyo soil and dust samples. Of the 19 soil and dust samples from Tokyo, we were able to measure the radioactivity of six samples. The radioactivity ranged from 50.9 Bq/kg to 338.3 Bq/kg. The mean activity of ^{137}Cs was 130.2 Bq/kg with a standard deviation of 117.6 Bq/kg. The results showed that soil samples from Tokyo were the least radioactive among the five sample sets.

Figure 11: Activity of ^{137}Cs in Tokyo soil and dust samples.

4.3.3 Azuma Sports Park Sample

Of the 13 samples from the Azuma Sports Park, we were able to measure the radioactivity of five samples. The radioactivity ranged from 78.1 Bq/kg to 6176.0 Bq/kg. The mean radioactivity is 2703.9 Bq/kg with a standard deviation of 2729.8 Bq/kg. The mean radioactivity of this sample set was 20.7 times higher than the mean radioactivity of the Tokyo sample set.

Figure 12 showed the activity of ^{137}Cs in Baseball court soil and dust samples. Only four plotted samples appear in Fig 12 because one sample was an infield dirt with no recorded location. The mean radioactivity of the Azuma Sports Park sample set was the second least radioactive set among the five sets.
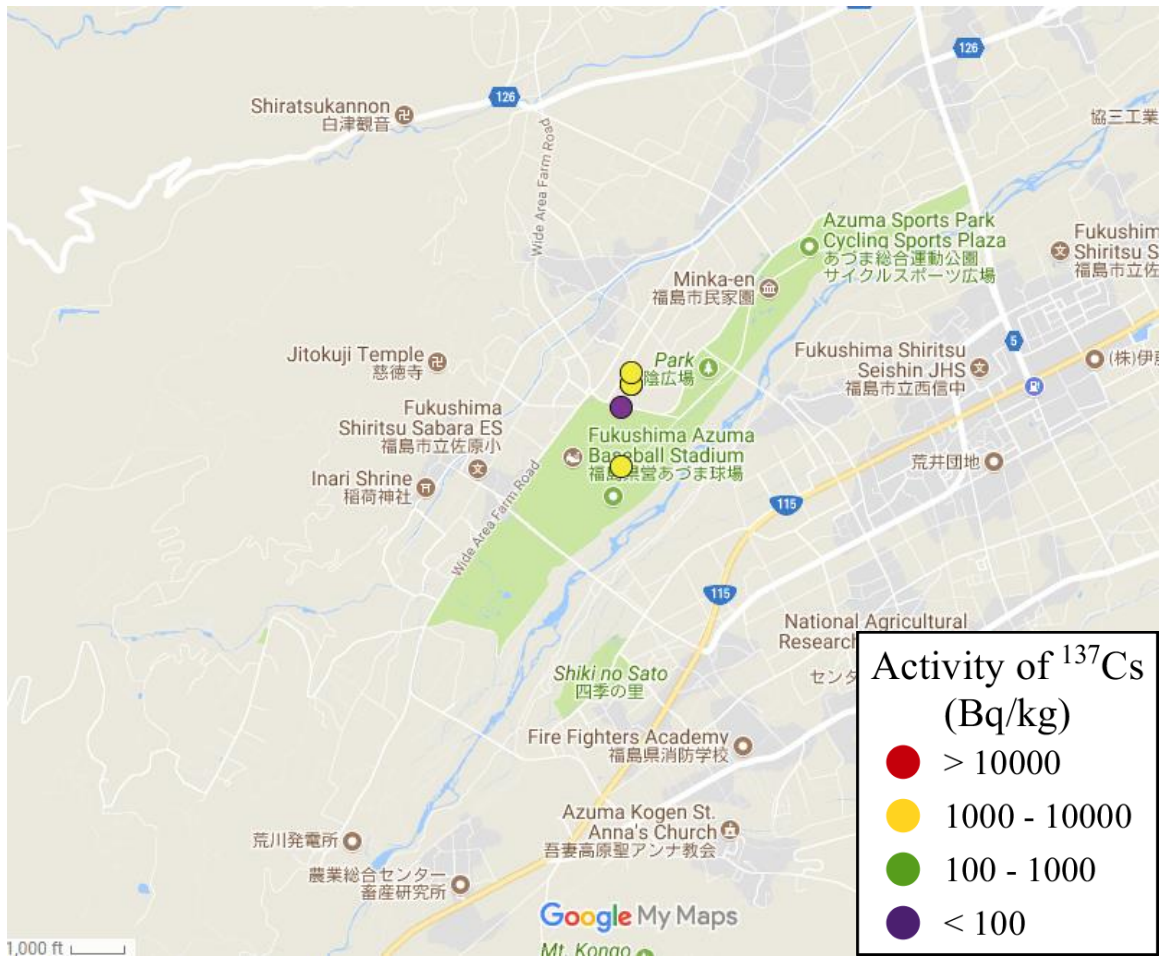
Figure 12: Activity of 137Cs in Azuma Sports Park soil and dust samples.

4.3.4 Tourist Route Sample

Of the 18 soil and dust samples from the Tourist route samples, we were able to measure the deposition of ^{137}Cs in five samples. The radioactivity ranged from 1138.8 Bq/kg to 10831.7 Bq/kg. The mean radioactivity is 3206.0 Bq/kg (σ = 4266.7 Bq/kg). The mean radioactivity of the Tourist route sample was 24.6 times higher than that of the Tokyo sample.
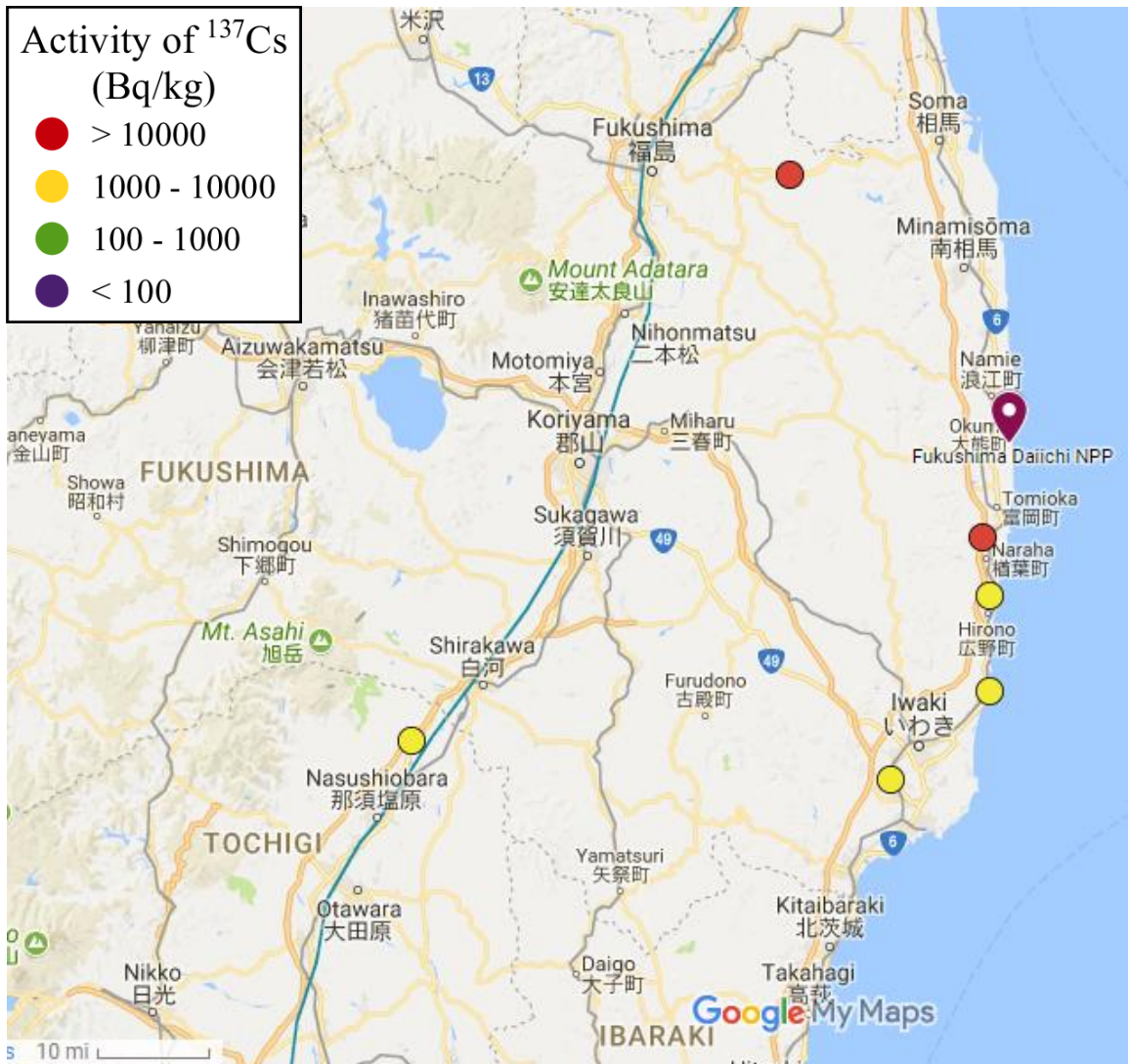
Figure 13: Activity of 137Cs in tourist route soil and dust samples.

4.3.5 Proposed torch route sample

Figure 14 showed the radioactivity of ^{137}Cs in the proposed torch route soil and dust samples. Of the 31 samples from the tourist route, we were able to measure 13 samples. The proposed torch route sample was the most radioactive sample set and had the greatest variance among the three previous sample categories. The radioactivity ranged from 38.6 Bq/kg to 28041.5 Bq/kg. The mean radioactivity was 7896.0 Bq/kg (σ = 8103.9 Bq/kg). Seven samples (7 of 13) exceeded the mean radioactivity.

The mean radioactivity of the proposed torch route sample was 60.6 times higher than that of Tokyo sample.
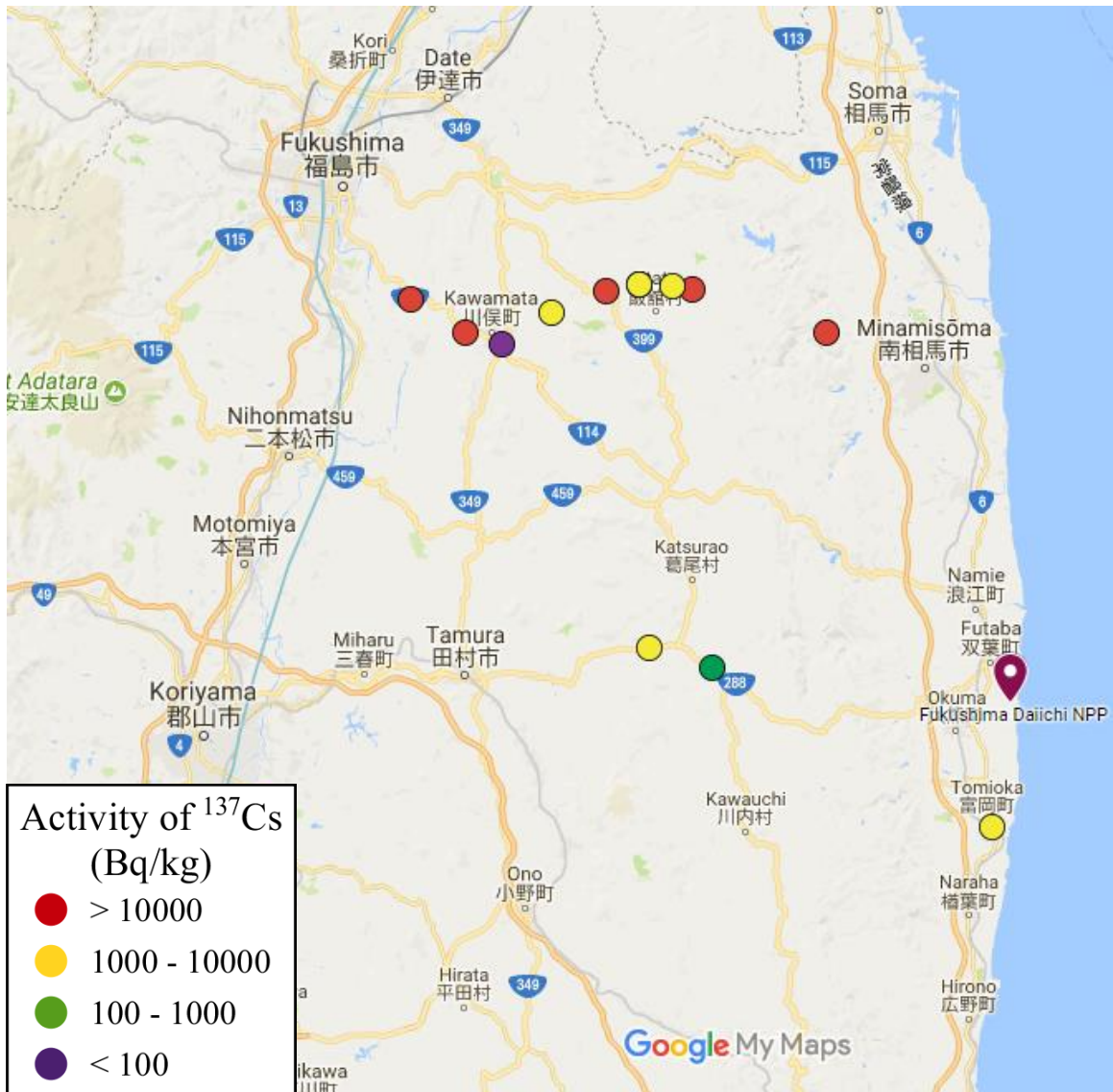
Figure 14: Activity of ^{137}Cs in proposed torch route soil and dust samples.

4.3.6 Non-Olympic sample

Of the seven Non-Olympic sample, we were able to measure the radioactivity of one sample located at the Entrance to Fukushima Dai-ichi NPS waste mounds. The activity of ^{137}Cs of this sample was 14119.8 Bq/kg, 88.2 times higher than the mean radioactivity of the Tokyo sample set. There is high activity of ^{137}Cs in this sample, explained by its close proximity to the Fukushima Nuclear Power Plant.
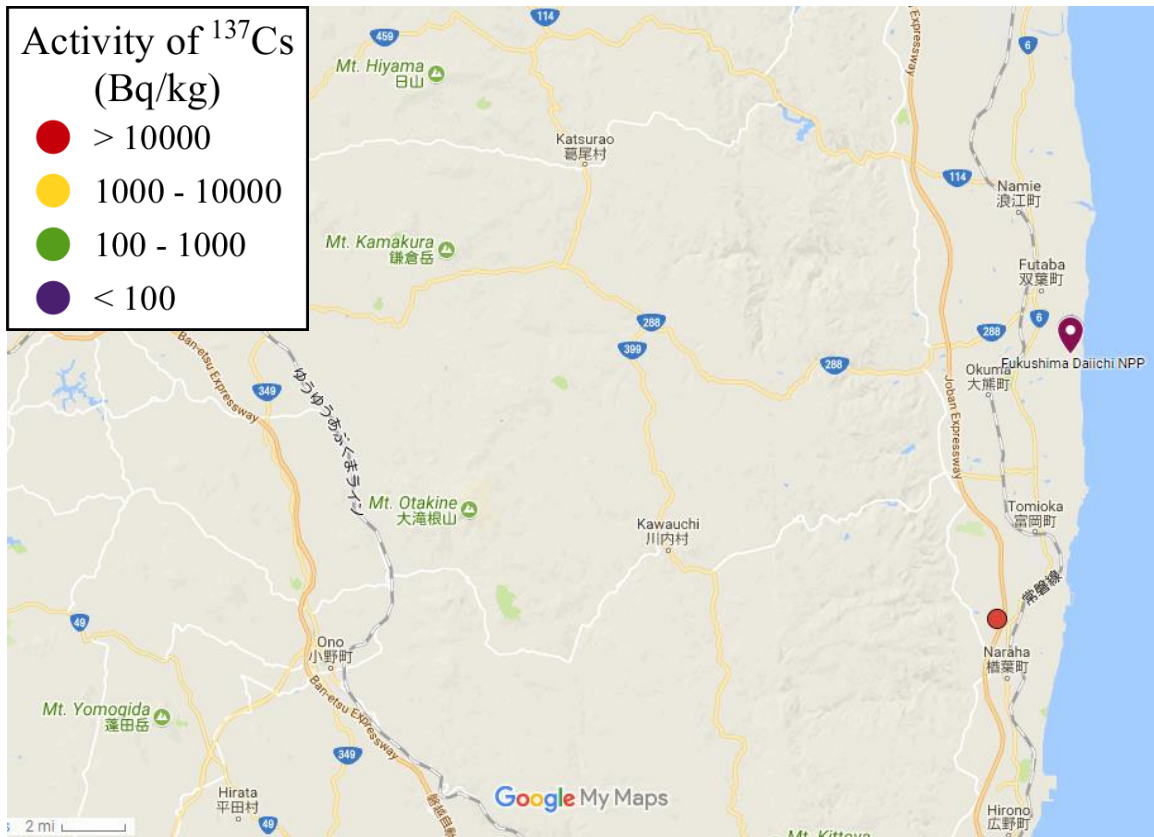
Figure 15: Activity of ^{137}Cs in Non-Olympic soil and dust sample.

5 Discussions and Recommendations

5.1 Discussions

The results support our initial assumptions that samples that originate within the Fukushima Prefecture possess a much higher concentration of radioactive material than those further away. Especially over the years, although there has been numerous research done on measuring the radioactivity of Japan soil, it was unclear whether the public's health was at risk. Through five months of researching and testing, this study provides the amount of radiation detected in the gathered soil and dust samples. These findings give a template to determine any long-term health risks associated with these measured values. Examples of the amount of cesium-137 exposed to people in everyday life provides a reference to our results. The findings showed that the Tokyo sample set had the lowest radioactivity level, which was understandable based on its significant distance from the Fukushima Nuclear Power Plant. On the contrary, the proposed torch route samples had the highest mean radioactivity due to their close proximity to the plant. Based on the measurement, we estimated qualitatively that the radiation exposure of people living near the Azuma Sports Park area was 20.7 times higher than that of people living in Tokyo. The main tourist and proposed torch routes had radiation exposure of 24.6 and 60.6 times higher, respectively, than in Tokyo. Although most of the radiation decayed rapidly following the initial disaster and has decreased minimally throughout the following years, the significantly high amount of Cesium-137 in the proposed torch route area showed concerns about public health.

Our studies seek to compare the results with previous studies. Kaltofen et al. isolated and analyzed the activity of radiocesium in 180 dust and soil samples from Japan, showing a high mean radioactivity of 25.7 kBq/kg among the sample set (2017). The results was 5.2 times higher than our mean radioactivity and the difference was understandable because of the difference in sampling criteria. While Kaltofen et al. focused on identifying the hot spots within the area around the Fukushima Prefecture, our groups measured samples that were further away from the Fukushima Nuclear Power Plant.

The results in this study were in agreement with Saito et al., who reported a much higher deposition of Cesium-137 in the area to the northeast of the Fukushima Nuclear Power Plant and the further away from the plant, the lower the deposition of Cesium-137 (2015). Accordingly, our results showed that the highest radioactivity level was at the proposed torch route, which is located to the northeast of the plant. The further away from the plant for example, in Tokyo and the Azuma Sports Park, the lower the activity of Cesium-137. However, because of the differences in sampling techniques and reported unit of radioactivity, there could not be an established direct comparison.

With the 2020 Olympics hosted in Japan, our study will benefit officials when they decide whether the radioactivity level at the Olympic venues are acceptable. The map created also gives a quantitative summary of our findings, which estimates the actual dose that people living in these areas may receive. Tourism and agriculture can benefit from our data by creating a simple guide to the danger areas around Japan. This can heavily tie into economic situations as well.

5.2 Limitations and Follow-up study

Through measuring the radioactivity of the samples and comparing our results with published work, we were able to complete the project. The activity map of Cs-137 in Japan soil was created. There were, however, limitations in our study that discusses suggestions on further research.

The first obstacle that we faced in this study was the large number of samples collected from Japan. Moreover, there was no clear suggestion on which sample to start with so at the beginning of the project, samples were selected randomly. A direct consequence for the random selection was that we could not measure all the samples within one set because of the time constraint and measured samples were in different sets. Therefore, if we had a more concrete approach, we would be able to have a better mechanistic understanding of the activity of Cesium-137 in Japan soil.

The second limitation was the number of samples that we were able to measure in this project. As shown in the findings, the radioactivity varied enormously even within one sample set. Therefore, if we were able to measure the radioactivity of more samples, a better radioactivity mean for each sample set would be collected.

The third limitation of the project was the mapping process. Google Map was an acceptable software, but the control of information presented on Google Map was limited. For example, the size of the icon that we used in the mapping could not be decreased, which resulted in large and overlapping icons. Therefore, we were not able to show all the data points on the overall activity map. In short, we learned that there is software that allows better controlling in the map-making process, but due to our limitation in coding techniques, Google Maps was the only viable choice for this project.

From the limitations that we learned from this project, the following studies allowed a better understanding of the activity of Cesium-137 in Japan soil:

- Measure the radioactivity of samples in on sample set instead of random selection. This will save time and yield a more concrete result for each set.
- Have a detailed schedule for measuring the radioactivity. Because each sample was measured for three hours, only three samples could be measured in one day or equivalent of one sample a day. If the rate of measuring is lower than this, it will take a much longer time to go through all the samples.
- Use a different software for mapping process. Example of software to use is Mapbox, which requires knowledge on JavaScript to execute.

5.3 Summary

This project aimed to study the activity of Cesium-137 in soil and dust samples from Japan as the consequence of the Fukushima Dai-ichi nuclear disaster in March 2011. The goals of the project were to measure and analyze the radioactivity at different locations in Japan, generate a map to illustrate the radioactivity level in Japan soil, and qualitatively estimate human exposure to radioactivity.

The employment of various study methods and experiment designs completed the objectives. Through literature review and discussion with advisors and lab instructors, the methodology allowed for measurement and analysis on the radioactivity of Cesium-137 in the samples. We were able to measure the radioactivity of 30 samples and used the results to create the Cesium-137 activity map using Google Map.

The measured results showed a much higher activity of Cesium-137 in the proposed torch route compared to other areas. Overall, the further away from the Fukushima Dai-ichi Nuclear Power Plant, the lower the radioactivity. The activity of Cesium-137 in Tokyo, the furthest site from the plant, was the lowest when compared to the other sites. Therefore, the activity of Cesium-137 in Tokyo sample was used as the baseline to qualitatively estimate the human exposure to radiation. Upon measuring and analyzing, we compared our results to the literature and published work to validate our data.

Furthermore, these results uses cross-references with the agriculture regulation amount of Cs-137 in the soil. The value for radioactivity of Cesium-137 in soil must be below 5000 Bq/kg. At the Azuma Sports Park, the soil and dust samples yielded a range of 78.1 Bq/kg to 6176.0 Bq/kg. This particular Olympic venue is around 90 km from the Nuclear Power Plant. The other sites that are closer to the Nuclear Power Plant like the tourist route, proposed torch route, and non-Olympic samples have higher amounts due to the close proximity to ground zero of the disaster.

5.4 Recommendations and Suggestion for Follow Up Studies

From the results of our study, we observed that areas in and close to the Fukushima prefecture exhibit a high concentration of radioactive fallout. Past and current tests show the locations of high amounts of radiation at the locations, which originate close to the original site of the disaster. Furthermore, the results showed a significantly higher amount of radioactive materials in the proposed torch route compared to those in Tokyo.

Given the results from testing, we confidently make the following recommendations:
1. Further study on the activity of Cesium-137 on the proposed torch route is necessary to understand how much radioactive materials remain.
2. A more detailed study with more soil and dust samples can give a more accurate map of specific areas of interest.
3. Olympic officials should consider using the results of this project to decide whether the radioactivity level at the proposed torch route and the Olympic venues are within acceptable level.
4. Qualified health professionals should use this data to make connections about short and long-term effects on health.

References

Agency for Toxic Substances and Disease Registry (2015, January 21). Toxic Substances Portal Cesium. Retrieved March 02, 2018, from https://www.atsdr.cdc.gov/toxprofiles/TP.asp?id=578&tid=107

Atomic Energy Society of Japan (AESJ). Atomic Energy Society of Japan, SpringerLink (Online service), & Springer Books. (2015;2014;).

The Fukushima Dai-ichi nuclear accident: Final report of the AESJ investigation committee (2015th ed.). Tokyo: Springer Japan.10.1007/978-4-431-55160-7

Dersee,Thomas & Pflugbeil, Sebastian (2011). *Calculated Fatalities from Radiation Officially Permissible Limits for Radioactively Contaminated Food in the European Union and Japan*. Retrieved from https://www.foodwatch.org/uploads/tx_abdownloads/files/fw_report_CalculatedFatalities fromRadiation11_2011.pdf

Evacuation Orders and Restricted Areas. (2017, March 31). Retrieved March 02, 2018, from http://fukushimaontheglobe.com/the-earthquake-and-the-nuclear-accident/evacuation-orders-and-restricted-areas

Epstein, Edward Jay. "What Was Lost (and Found) in Japan's Lost Decade." *The Hive*, Vanity Fair, 24 Feb. 2016, www.vanityfair.com/news/2009/02/what-was-lost-and-found-in-japans-lost-decade.

Foodwatch (2011, September 19). Calculated Fatalities from Radiation - Officially Permissible Limits for Radioactively Contaminated Food in the European Union and Japan. Retrieved March 02, 2018, from https://www.foodwatch.org/foodwatch-report-calculated-fatalities-from-radiation/

Future From Fukushima (2018, February 1). Estimated population in Fukushima Prefecture. Retrieved March 02, 2018, fromhttps://www.pref.fukushima.lg.jp/sec/11045b/15846.html

Jnto Japan: The Official Guide. Japan National Tourism Organization. Retrieved March 03, 2018, from https://www.jnto.go.jp/eng/regional/fukushima/index.html

International Nuclear and Radiological Event Scale (INES). (2017, November 22). Retrieved March 02, 2018, from https://www.iaea.org/topics/emergency-preparedness-and-response-epr/international-nuclear-radiological-event-scale-ines

Kaltofen, M., & Gundersen, A. (2017). Radioactively-hot particles detected in dusts and soils from northern japan by combination of gamma spectrometry, autoradiography, and SEM/EDS analysis and implications in radiation risk assessment. Science of the Total Environment, 607, 1065-1072. doi:10.1016/j.scitotenv.2017.07.091

Kato, H., Onda, Y., & Teramage, M. (2012;2011;). Depth distribution of 137Cs, 134Cs, and 131I in soil profile after fukushima dai-ichi nuclear power plant accident. Journal of Environmental Radioactivity, 111, 59-64. doi:10.1016/j.jenvrad.2011.10.003

Kinoshita, N., Sueki, K., Sasa, K., Kitagawa, J., Ikarashi, S., Nishimura, T., . . . Yamagata, T. (2011). Assessment of individual radionuclide distributions from the Fukushima nuclear accident covering central-east japan. Proceedings of the National Academy of Sciences of the United States of America, 108(49), 19526-19529. doi:10.1073/pnas.1111724108

Knoll, G. F. (2010). Radiation detection and measurement (4th ed.). Hoboken, N.J: John Wiley.

Kyodo. "Tens of Thousands Flock to the Imperial Palace for Annual Viewing of Autumn Foliage." *The Japan Times*, 6 Dec. 2015, www.japantimes.co.jp/news/2015/12/06/national/tens-of-thousands-flock-to-the-imperial-palace-for-annual-viewing-of-autumn-foliage/.

Marks, Shannon. "Facts on the Imperial Palace." *USA Today*, Gannett Satellite Information Network, traveltips.usatoday.com/imperial-palace-9888.html.

Morino, Y., Ohara, T., & Nishizawa, M. (2011). Atmospheric behavior, deposition, and budget of radioactive materials from the Fukushima Dai-ichi nuclear power plant in march 2011. Geophysical   Research Letters, 38(7), n/a. doi: 10.1029/2011GL048689

Nagao, S., Kanamori, M., Ochiai, S., Tomihara, S., Fukushi, K., & Yamamoto, M. (2013). Export of (134) Cs and (137) Cs in the Fukushima river systems at heavy rains by typhoon Roke in September 2011. Biogeosciences, 10(10), 6215-6223. doi:10.5194/bg-10-6215-2013

Nuclear Power in Japan. (2017, December). Retrieved March 02, 2018, from http://www.world-nuclear.org/information-library/country-profiles/countries-g-n/japan-nuclear-power.aspx

Ohno, T., Muramatsu, Y., Miura, Y., Oda, K., Inagawa, N., Ogawa, H., . . . Sato, M. (2012). Depth profiles of radioactive cesium and iodine released from the Fukushima Dai-ichi nuclear power plant   in different agricultural fields and forests. Geochemical Journal, 46(4), 287-295. 10.2343/geochemj.2.0204

Radiation and Life. (2012, December). Retrieved March 02, 2018, from http://www.world-nuclear.org/information-library/safety-and-security/radiation-and-health/radiation-and-life.aspx

Saito, T., Saito, K., Tanihata, I., Fujiwara, M., Shimoura, S., Otsuka, T., . . . Shibata, T. (2015;2014;). Detailed deposition density maps constructed by large-scale soil sampling for gamma-ray emitting radioactive nuclides from the Fukushima Dai-ichi nuclear power plant accident. Journal of Environmental Radioactivity, 139, 308-319. doi:10.1016/j.jenvrad.2014.02.014

Shoebridge, G. (2012, January 6). Electric Car Conversion Blog. Retrieved March 02, 2018, from http://www.gavinshoebridge.com/news/basic-guide-to-radiation-levels-in-%C2%B5svh-and-msvh/

Tanaka, K., Takahashi, Y., Sakaguchi, A., Umeo, M., Hayakawa, S., Tanida, H., . . . Kanai, Y. (2012). Vertical profiles of iodine-131 and cesium-137 in soils in Fukushima prefecture related to the Fukushima Dai-ichi Nuclear Power Station Accident. *Geochemical Journal, 46*(1), 73-76. doi:10.2343/geochemj.1.0137

The number of Fukushima children diagnosed with or suspected to have thyroid cancer became 172. (2016, June 07). Retrieved March 02, 2018, from

http://fukushimaontheglobe.com/the_earthquake_and_the_nuclear_accident/health-and-medical-services/4625.html

Tomoko M. Nakanishi; Agricultural implications of the Fukushima nuclear accident, Journal of Radiation Research, Volume 57, Issue S1, 1 August 2016, Pages i47–i52, https://doi.org/10.1093/jrr/rrw042

Turner, J. E. (2008;2007;). Atoms, radiation, and radiation protection (1. Aufl.;3rd completely rev. and enlarg;3; ed.). Hoboken: Wiley-VCH.

Tokyo Area – Japan National Tourism Organization, (2014). "The Imperial Palace Area - Japan National Tourism Organization." *Japan National Tourism Organization Web Site*, Japan National Tourism Organization, www.jnto.go.jp/eng/regional/tokyo/imperial.html.

"Tokyo Imperial Palace• Historic Site in Tokyo." *Tokyo Imperial Palace*, Japan Guide, www.japan-guide.com/e/e3017.html.

Wang, Y., Morita, S., Kataoka, N., Imaizumi, H., & Kano, N. (2016, October 15). Observation of Tritium Behavior Both in Monthly Precipitation in Niigata City and in Spring Water at Top of Mt. Zao and Some Mountains in Fukushima Prefecture After the Fukushima Dai-ichi Nuclear Power Plant Accident. Retrieved March 02, 2018, from https://www.jstage.jst.go.jp/article/radioisotopes/65/10/65_651002/_article

World Cities Forum, "Number of International Tourists per Year." *World Cities Culture Forum*, World Cities Culture Forum, www.worldcitiescultureforum.com/data/number-of-international-tourists-per-year.

Yasunari, T., Stohl, A., Hayano, R., Burkhart, J., Eckhardt, S., & Yasunari, T. (2011). Cesium-137 deposition and contamination of Japan soils due to the Fukushima nuclear accident. *Proceedings of the National Academy of Sciences of the United States of America, 108*(49), 19530-19534. Retrieved from http://www.jstor.org.ezproxy.wpi.edu/stable/23059528

Appendix A. Sample Preparation

Figure 16: Samples drying by keeping them open to ambient air in one week (62.2 °F, 22% humidity and 1 atm)
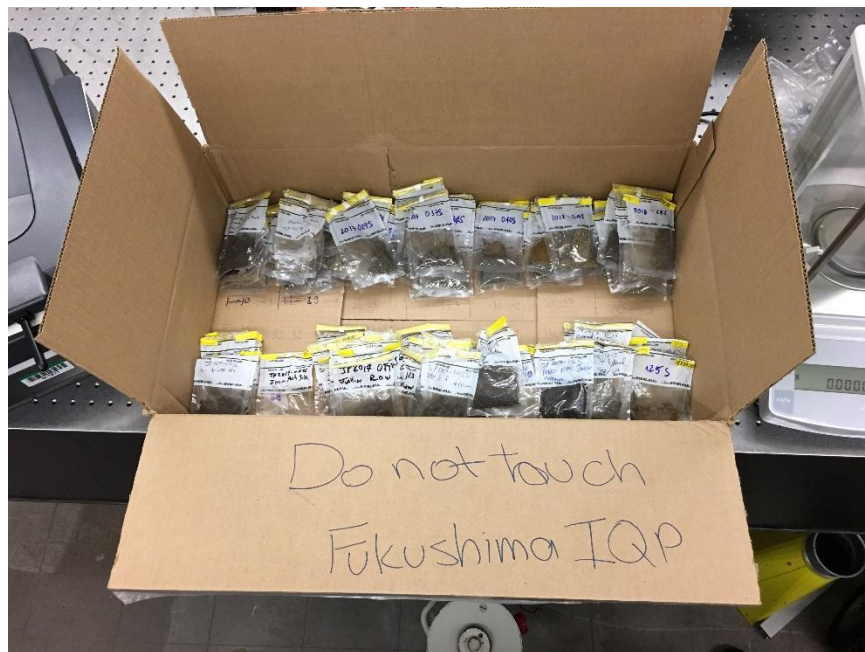

Figure 17: Sample ordering. After the drying process, samples were sorted based on their name.

Appendix B. Equipment

Figure 18: Sodium Iodide (NaI) detector.

Appendix C. Efficiency Measurement and Blank Measurement

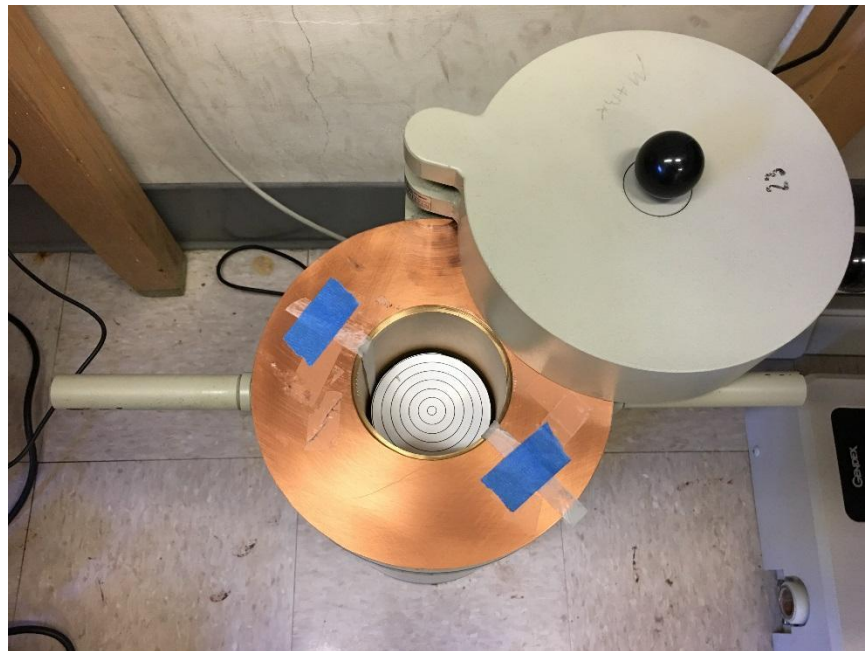Figure 19: Cesium-137 in a Whirlpak® bag.

Figure 20: Sodium iodide (NaI) detector surface was divided into seven concentric zones.

Figure 21: Efficiency measurement setup.
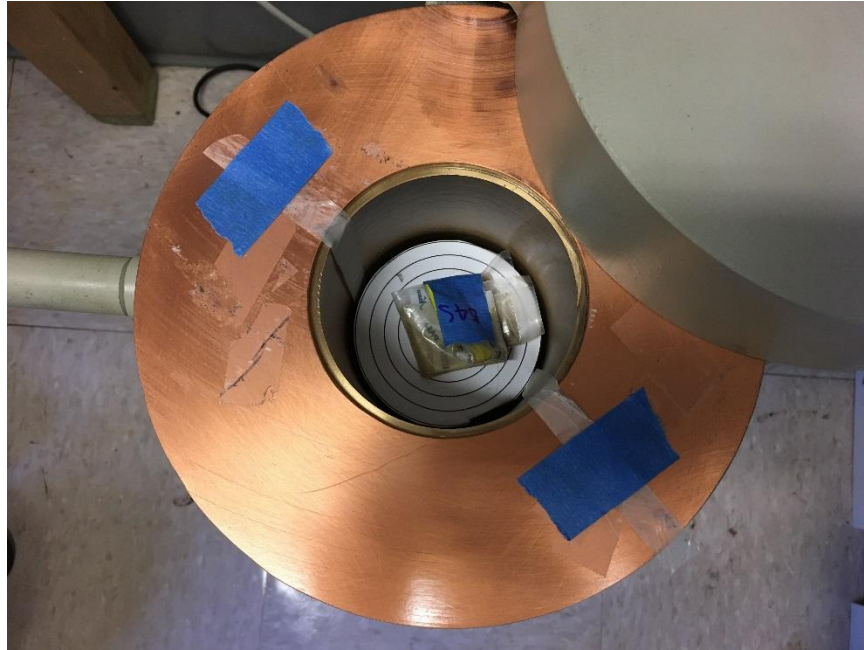

Figure 22: Background measurement setup.

Appendix D: Sample Measurement

Figure 23: Sample measurement setup.